# Chapter 13

# Water Vapor Observations in the ARM Program

D. D. TURNER

*NOAA/National Severe Storms Laboratory, Norman, Oklahoma*

E. J. MLAWER

*Atmospheric and Environmental Research, Inc., Lexington, Massachusetts*

H. E. REVERCOMB

*Space Science and Engineering Center, University of Wisconsin–Madison, Madison, Wisconsin*

## 1. Introduction

From the earliest days of the ARM Program, water vapor and temperature measurements were considered among the highest priority measurements made at the ARM sites. The program founders recommended that these observations "be performed on a continuing, real-time basis throughout the experiment" so that the radiation models and cloud parameterizations could be evaluated over a wide range of atmospheric conditions (DOE 1990; ARM 2016, appendix A). Furthermore, the program founders believed that these measurements should be made on a time scale appropriate for the study of radiative properties, which necessitated a temporal resolution on the order of minutes (DOE 1990).

In the early 1990s, many different instruments were available to provide information on the atmospheric water vapor concentration and temperature. Some of these instruments had been used for years in the operational community (e.g., radiosonde and in situ sensors), whereas some were very much research instruments (e.g., Raman lidars, global positioning systems, and microwave radiometers). However, because of the critical need to measure water vapor with the precision necessary to improve the accuracy of radiative transfer models, the program decided to deploy multiple instruments sensitive to water vapor at each site. This strategy provided opportunities to compare the different technologies and develop new methods to combine observations to create more accurate water vapor products.

This chapter details the history and evolution of water vapor measurements within the ARM Program. Most of the early work focused around the needs of the Instantaneous Radiative Flux (IRF) working group within the ARM science team. The IRF was striving to advance the work started with the Intercomparison of Radiation Codes in Climate Models (ICRCCM; see Ellingson et al. 2016, chapter 1): namely, the evaluation and improvement of the accuracy of detailed radiative transfer models used to build radiation parameterizations used in climate models. Although temperature observations are just as critical to advance ARM science, the uncertainties in temperature observations were considered smaller and less important and, consequently, received less attention in the earlier days of the program.

## 2. The earliest days

In the early years of the program, the IRF was arguably the most organized working group because 1) the Spectral Radiance Experiment (SPECTRE) science objectives were a large part of the ARM science plan (Ellingson and Wiscombe 1996; Ellingson et al. 2016, chapter 1); 2) the instruments needed to accomplish some of the IRF goals, in particular the Atmospheric Emitted Radiance Interferometer (AERI), were already available and were among the first instruments deployed at the Southern Great Plains (SGP) site; and 3) a large fraction of the IRF membership participated

*Corresponding author address*: D. D. Turner, NOAA/National Severe Storms Lab, Forecast Research and Development Division, National Weather Center, 120 David L. Boren Blvd., Norman, OK 73072.
E-mail: dave.turner@noaa.gov

DOI: 10.1175/AMSMONOGRAPHS-D-15-0025.1

in SPECTRE and thus were already familiar with each other and the datasets they would analyze.

The original goal established by the IRF, because of the instrumentation available in the early 1990s, was to improve the accuracy of clear-sky infrared radiative transfer models, and in particular, the water vapor continuum model component [see Turner and Mlawer (2010) for a simple overview of the water vapor continuum, or Mlawer et al. (2012) for a more detailed discussion]. Toward this end, the IRF developed the idea of the Qualitative Measurement Experiment (QME; Turner et al. 2004). The QME was a radiance closure experiment designed to evaluate three critical components simultaneously: 1) the spectral radiance observations, 2) the radiative transfer model, and 3) the temperature and humidity observations, as well as any other observations required by the radiative transfer model. While there were several QMEs defined by the IRF, the primary one compared AERI spectral downwelling radiance observations (Knuteson et al. 2004a,b; see the appendix) against those computed by the Line-by-Line Radiative Transfer Model (LBLRTM; Clough et al. 1992, 2005). A large number of IRF and ARM infrastructure members would work on this closure exercise for over a decade (Turner et al. 2004). The next chapter in this monograph (Mlawer and Turner 2016, chapter 14) provides additional details about the AERI/LBLRTM QME effort and some of the significant improvements made as a result of those activities.

The initial challenge of this QME was which, if any, of the three components of this radiative closure study could be trusted enough to serve as a foundation for evaluating the other components. In many ways, the QME is like building a three-legged stool; if any of the legs are weak or insufficient, then the stool will not stand properly until that leg is improved. The original QME idea (Miller et al. 1994) proposed to take advantage of portions of the electromagnetic spectrum with better-known (i.e., less uncertain) spectroscopy, which, together with the perspective that the measurement–calculation results should be spectrally consistent, would provide a suitable basis to evaluate the observations used in the QME. Then, after there was confidence that the observations were good, improvements could be made to the radiative transfer model itself. Key to this approach was a robust approach to specifying the thermodynamic profile in the radiating column above the AERI.

The original programmatic desire was that the thermodynamic profile observations that would be used as input to the LBLRTM would come from the Raman lidar and radio acoustic sounding system (RASS; May et al. 1988). These instruments are active profiling systems, meaning that they transmit electromagnetic energy and observe the backscattered signal, which is then calibrated to provide profiles of water vapor and virtual temperature, respectively. Even though these systems take advantage of radiative transfer principles, these observations were considered independent of uncertainties that affect radiative transfer models in general circulation models (GCMs). However, it would take many years before the Raman lidar was developed fully into an operational system (Turner et al. 2016, chapter 18), and the ability of the RASS to provide temperature profiles over much of the troposphere was never truly realized. Thus, the ARM Program, and the IRF in particular, depended heavily on the radiosondes launched by the program. However, radiosondes turned out to have their own issues with respect to reliability and accuracy.

## 3. Characterizing the radiosonde and MWR

One of the earliest comparisons done to assess water vapor measurements was to compare the precipitable water vapor (PWV) measured by the ascending radiosonde with that retrieved from the two-channel ARM microwave radiometers (MWRs). This was, in fact, the first QME; the radiosonde profile was input to a microwave radiative transfer model, and the calculated brightness temperatures were compared to those measured by the MWR. The multiyear coincident observations from the MWR and radiosondes (and the AERI) would turn out to be very important for truly characterizing these sensors.

The comparisons of PWV from the MWR and radiosonde demonstrated significant bias between the two instruments, again bringing to the forefront the question of which components of this QME could be trusted. Initially, this PWV bias, which could be 10% or more, was attributed to errors in the radiative transfer model used to invert the MWR's brightness temperatures to PWV, and thus tuning functions were developed and applied to the MWR observations (Liljegren 1994). These tuning functions were linear functions used to modify the observed brightness temperatures to account for supposed deficiencies in the microwave water vapor absorption model, and were determined typically from a large number of clear-sky radiosonde/MWR observations. However, it seemed that the tuning functions needed to change with some periodic interval, and thus there were questions about whether this was really an issue with the absorption model[1] or if it was

[1] The program was using the Liebe and Layton (1987) model for gaseous absorption in the microwave portion of the spectrum at the time. The other commonly used model at the time was Rosenkranz (1998). Tony Clough and his colleagues would subsequently develop the MonoRTM for the microwave region of the spectrum with ARM support (Clough et al. 2005; Payne et al. 2008), and this would eventually become the primary microwave absorption model used by the program (e.g., Turner et al. 2007).

due to changes in the calibration in either the MWR or perhaps the radiosonde.

Tony Clough was a strong voice in the IRF who advocated that the absorption model was accurate and was not responsible for the differences in the PWV between the sonde and MWR. He had performed laboratory measurements to measure the Stark effect and was able to determine that the strength of the 22.2-GHz water vapor absorption line (which is the water vapor spectral feature that was being observed by the ARM MWRs) was known to better than 1% (Clough et al. 1973). Furthermore, PWV is more sensitive to MWR-measured downwelling radiation at 23.8 GHz, which is on the side of the 22.2-GHz water vapor line, than its measurement at 31.4 GHz, which is in a window between absorption lines. The 23.8-GHz observation is close to the ''hinge'' point of the 22.2-GHz water vapor absorption line, and thus the modeled downwelling radiance at 23.8 GHz is relatively insensitive to errors in the half-width of this absorption line. For these reasons, Tony Clough argued that the differences between the PWV observed by the MWR and radiosondes were due to instrument calibration.

It had become clear that uncertainty in the PWV was the limiting factor in improving the accuracy of the infrared radiative transfer models (Revercomb et al. 2003). The need to greatly improve the accuracy of the water vapor observations, and in particular the PWV measurements, led to the development and execution of a series of water vapor intensive observation periods (WVIOPs) by the ARM Program. These WVIOPs, which were led by Hank Revercomb, occurred at the SGP site in 1996, 1997, 1999, and 2000 and brought a wide range of different instruments to the site to help characterize the accuracy and precision of operational and experimental instruments (Revercomb et al. 2003).

The WVIOPs, together with the operational nature of the ARM Program that collected a massive amount of coincident observations over many years, helped to improve the accuracy of these water vapor measurements. The improvements spanned many aspects of the measurement problem: better understanding of instrument biases, calibration improvements, retrieval algorithm and forward model improvements, improvements in sampling, and more. Indeed, the discussions among the WVIOP participants during the ARM science team meetings and fall working meetings in the mid-to-late 1990s were far ranging and exciting, and it took several years to fully appreciate how the many changes worked together to improve the overall accuracy of all of the water vapor observations.

The simultaneous side-by-side comparison of many MWRs was one of the activities that occurred during the WVIOPs. Jim Liljegren, the MWR instrument mentor at the time, deployed up to six of the ARM two-channel MWRs side by side to evaluate the consistency of the measurements from these systems (Revercomb et al. 2003). Ed Westwater, an ARM science team member, deployed his large trailer-based MWR at the site also. These activities demonstrated that small details, such as ensuring that the radiometer was level and accounting for the finite beamwidth of the radiometer, were important to obtaining accurate calibrations from the tip-curve technique (Han and Westwater 2000), which was used to determine the calibration of all of the ARM MWRs in the field. Jim Liljegren incorporated these ideas, together with additional findings on the temperature-dependent aspects of the calibration, into a new algorithm to automatically (without human intervention) calibrate the MWRs (Liljegren 2000). These advances in the MWR calibration removed small biases but, more importantly, created a dataset that was consistently calibrated over time by removing the subjective elements from the process.

The long-term collocated MWR and radiosonde dataset also highlighted several problems with the radiosonde measurements. In particular, an early analysis by Jim Liljegren and Barry Lesht (the radiosonde instrument mentor) demonstrated that factory calibration errors could impact the accuracy of radiosonde humidity measurements. ARM has always utilized Vaisala radiosondes, starting with the RS80-H, transitioning to the RS90 in the early 2000s, and then to the RS92 around 2002. Vaisala calibrates dozens of radiosondes simultaneously in a batch at its factory, and because of the large number of sondes that ARM uses, ARM typically would receive many, or even all, of the radiosondes from a calibration batch. Liljegren and Lesht (1996), in an attempt to understand the differences between the sonde- and MWR-derived PWV values, separated PWV biases by the radiosonde serial number and discovered that one particular batch of sondes produced by Vaisala in the mid-1990s had a very poor humidity calibration. This finding spurred a deeper investigation, and significant mean bias differences (up to 20%) in the radiosonde calibration as a function of batch were found (Turner et al. 2003b; Fig. 13-1).

To better understand the bias between sonde and MWR PWV, many dual launches, where two radiosondes were flown on the same balloon in order to sample the same volume, were performed during the WVIOPs. These dual launches demonstrated that the humidity calibration of sondes from the same batch were generally in good agreement, with water vapor mixing ratio differences within 1%–2%, but that sondes from different calibration batches could have differences as

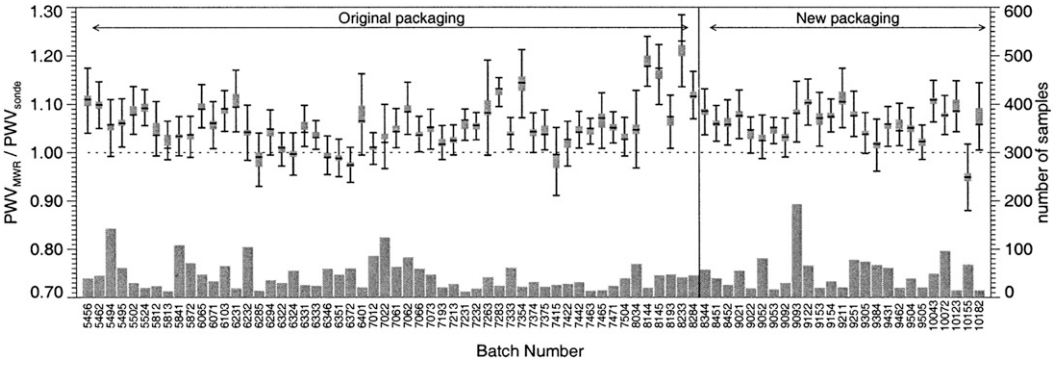


FIG. 13-1. Comparisons of the ratio of PWV from the MWR to that from the radiosonde from April 1994 to July 2000, separated by calibration batch, which shows the batch-to-batch variability of the results. Data are included only if the radiosonde achieved a height of at least 10 km, the cloud liquid water path was less than 50 g $m^{-2}$, and the number of samples in the batch was at least 10. The histograms at the bottom (gray bars) indicate the number of comparisons in each batch. The error bars indicate ±1 standard deviation about the mean, whereas the gray boxes are ±1 standard error of the mean. The thick black horizontal line is the median for each batch. The packaging of the radiosondes was changed midway through the period in an attempt to reduce/eliminate the dry bias, but it did not change the character of the differences. From Turner et al. (2003b).

great as 20% (Revercomb et al. 2003; Turner et al. 2003b). Figure 13-2 shows two dual-sonde examples that illustrate the differences in the moisture profiles from two sondes from different calibration batches. These dual launches suggested that the bias was to first order height independent, suggesting that the sonde data could be corrected by the use of a single-height independent scale factor. [The height-independent nature of the radiosonde humidity calibration bias was noted earlier by Ferrare et al. (1995), although the dataset at the time was not large enough to posit a hypothesis on the reason for the bias.] These findings agreed well with the findings by Wang et al. (2002), who determined that the source of the radiosonde humidity bias was due to outgassing of the RS80-H sonde packaging, which then effectively reduced the surface area of the capacitive humidity sensor (which would translate into a height-independent bias).

The dry bias induced by the radiosonde packaging was one source of error that was identified by the ARM Program during its WVIOPs. Another systematic error was discovered with long-term MWR versus sonde PWV comparisons. This activity demonstrated a diurnal difference in the bias between the two instruments, with the daytime results showing a larger bias (sonde more dry) than at night. The question at the time was simply the following: is there some temperature- or solar-energy-dependent calibration artifact impacting the accuracy of the MWR, or are the sondes the source of the issue? To investigate this issue, IRF members used comparisons between the AERI and the LBLRTM. The LBLRTM was used as a transfer standard, wherein radiosonde profiles were used as input to the model to compute downwelling radiance that could be compared to the AERI. Two sets of inputs were used to drive the LBLRTM: the original radiosonde profiles and radiosonde profiles where the humidity field was multiplied by a height-independent factor to yield the same PWV as was observed by the MWR. This resulted in two sets of infrared spectral residuals. Since the LBLRTM could potentially have spectral biases, the analysis would hinge more on the consistency of the spectral bias and RMS difference between daytime and nighttime results. [The focus on using the RMS difference to evaluate different inputs into a radiative transfer model would be used again when evaluating different cloud retrieval algorithms in radiative closure exercises (McFarlane et al. 2016, chapter 20).] The comparisons with the AERI demonstrated conclusively that the MWR was a stable instrument and that the diurnal difference between the sonde and MWR PWV was due to the radiosonde sensor (Turner et al. 2003b). Ultimately, this diurnal bias would be shown to be due to solar heating of the relative humidity sensor on the radiosonde (e.g., Vömel et al. 2007; Miloshevich et al. 2006; Miloshevich et al. 2009; Cady-Pereira et al. 2008).

## 4. The Rosetta Stone

While the program had come a long way in better understanding the radiosonde and the calibration of the MWR, there was still concern that the MWR-retrieved PWV may still be biased because a forward radiative transfer model was used to invert the observed brightness temperature observations to PWV. Thus, one of the primary objectives was to compare first-principle

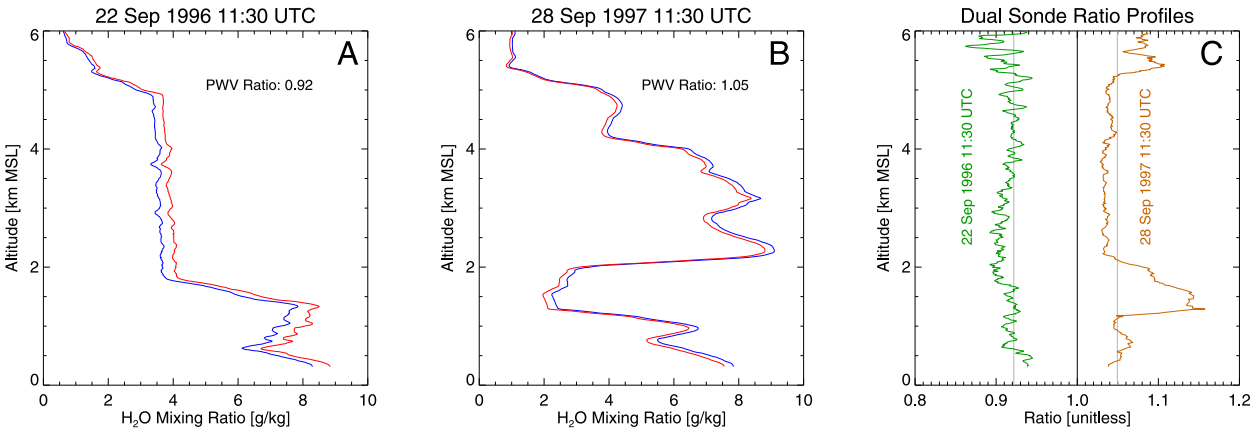


FIG. 13-2. The RH profiles from two radiosonde packages on the same balloon (i.e., a dual launch) at (a) 1130 UTC 22 Sep 1996 and (b) 1130 UTC 28 Sep 1997, where the radiosondes were from different calibration batches. (c) The ratio of these profiles [green and brown for the cases in (a) and (b), respectively] as a function of height.

measurement techniques in an attempt to define a ''rock'' that could serve as the reference for other observations.

Chilled-mirror hygrometers were considered to be one of these rocks, as the principle of the measurement is straightforward and related directly to the amount of water vapor in the atmosphere. This in situ sensor was not really designed for automated, long-term observations. However, the three-week comparisons during the 1996 and 1997 WVIOPs with another instrument, an in situ capacitive humidity sensor, at the surface demonstrated that well-maintained capacitive sensors could measure water vapor to better than 2% accuracy (Richardson et al. 2000). This result had two ramifications. First, since these capacitive in situ sensors are relatively cheap, the program installed two of these sensors for redundancy at both the 25- and 60-m levels on the tower at the SGP site. Second, because the radiosonde uses these same capacitive humidity sensors, the radiosonde variability was concluded not to be due to the sensor approach but rather to calibration, implementation of the sensor into the radiosonde package (e.g., should it have a cap to prevent wetting by cloud liquid or not), storage time, or other factors (Revercomb et al. 2003).

It was important to compare the two water vapor measurements that were thought to be accurate: traceable in situ sensors (chilled mirrors and capacitive sensors) on the tower and the PWV retrieved from the MWR based on underlying spectroscopy of the 22.2-GHz water vapor absorption line. To extend the in situ measurements throughout the column, the scanning Raman lidar from the National Aeronautics and Space Administration (NASA) Goddard Space Flight Center (GSFC) was used (Whiteman et al. 1992). This system, which played an important role in the development of the ARM Raman lidar (Turner et al. 2016, chapter 18), was able to scan in elevation and thus could make measurements directly next to the in situ sensors on the 60-m tower. Since the scanning Raman lidar, like the ARM Raman lidar, needs only a height-independent calibration factor, this factor was derived from the chilled-mirror hygrometer on the tower. The calibrated Raman lidar then collected zenith observations of water vapor mixing ratio, which were vertically integrated and compared to the PWV retrieved from the MWR. These observations were only done at night in cloud-free conditions during the WVIOPs, conditions under which the scanning Raman lidar was able to profile water vapor throughout the entire troposphere. The comparison, which spanned PWV values from less than 1 cm to over 4 cm, showed virtually identical agreement in water vapor sensitivity between the chilled-mirror hygrometer and MWR observations of the 22.2-GHz line with a slope of almost exactly 1.0 (Fig. 13-3; Revercomb et al. 2003). This finding was robust using both the statistical retrieval used in the mid-to-late 1990s by the ARM (red points in Fig. 13-3) and the newer physical retrieval developed in the early 2000s by Turner et al. (2007; blue points in Fig. 13-3). This finding was considered the ''Rosetta Stone'' that allowed the program to have faith in the accuracy of the MWR's PWV observations and to use these observations to begin the work of evaluating and improving the LBLRTM.

The demonstrated stability and accuracy of the MWR-retrieved PWV was a great boon for ARM science. The program began to scale all of its operational products to agree with the MWR in PWV. For example, the program created a value-added product called the Liebe-scaled sonde (LSSONDE; a new sonde data

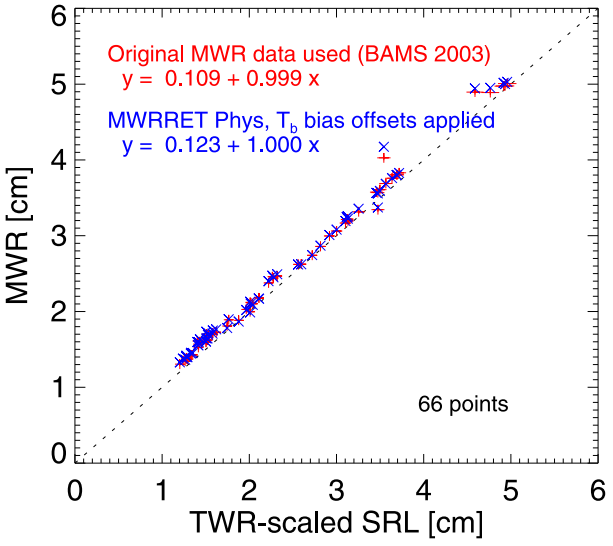


FIG. 13-3. The comparison of the MWR-retrieved PWV ($y$ axis) with PWV computed from the chilled-mirror calibrated NASA scanning Raman lidar ($x$ axis) during the 1997 WVIOP. The excellent agreement in sensitivity (i.e., the slope of exactly 1.0) demonstrated that these two first-principle measurements agreed and were termed the Rosetta Stone. From Turner et al. (2007).

product where the humidity profile was scaled to agree with the MWR), to use the MWR as the calibration source for the Raman lidar (Turner and Goldsmith 1999) and to scale all humidity profiles in its atmospheric state best-estimate value-added product (MERGESONDE) so that its PWV agreed with that value measured by the MWR.

## 5. Improving Arctic water vapor observations

The range of PWV at the SGP site is typically between 0.5 and 5.0 cm. This large dynamic range is due to the dry and cold Arctic airmass events that occasionally propagate that far south in the winter, as well as the occasional near-tropical-like events that come from the south in the summer. However, the typical radiometric uncertainty (i.e., random noise) in the MWR brightness temperature observations is 0.35 K, which translates into a PWV uncertainty of 0.025 cm (Turner et al. 2007); this is a relatively large percentage error for dry cases. At the North Slope of Alaska (NSA) site, the PWV can be as low as 0.1 cm, so the radiometric uncertainty in the MWR translates into a 25% random error. Since one of the primary objectives of the NSA site (Stamnes et al. 1999; Verlinde et al. 2016, chapter 8) was to evaluate the accuracy of infrared radiative transfer models in spectral regions such as the far-infrared that are normally opaque at typical midlatitude sites, more accurate values of PWV were needed than could be obtained from the MWR. For example, Tobin et al. (1999) noted that the strength of the foreign-broadened water vapor continuum model in the 17–26-$\mu$m spectral region was about three times too strong and made some modifications based upon data collected during the Surface Heat Budget of the Arctic Ocean (SHEBA) field campaign, but the 25% uncertainty in the water vapor observations resulted in approximately the same amount of uncertainty in the modeled strength of this absorption.

The program needed to have a more accurate water vapor measurement in the Arctic. Thus, there was a desire to conduct WVIOPs at the NSA site. Ed Westwater led the charge, with the support of many within the IRF. Tony Clough again was a forceful player, advocating for microwave radiometer observation on the 183.3-GHz water vapor absorption line. This line is significantly stronger than the 22.2-GHz water vapor line, and its strength is also known to better than 1% from Stark effect observations (Clough et al. 1973). The first Arctic WVIOP occurred in 1999 (Racette et al. 2005), a second in 2004 (Mattioli et al. 2007), and a third [under the auspices of the first Radiative Heating in Underexplored Bands Campaign (RHUBC)] in 2007 (Turner and Mlawer 2010). All three of these campaigns took place in the late winter (i.e., February–March), when the PWV is climatologically the lowest and the skies are more likely to be cloud free (thereby simplifying the analysis).

As was done during the WVIOPs at the SGP site, several guest instruments were operated at the NSA site to complement the operational ARM instruments. One guest instrument that was common in all three of these experiments was the National Oceanic and Atmospheric Administration (NOAA) ground-based scanning radiometer (GSR; Cimini et al. 2007). The first WVIOP also employed a NASA radiometer with multiple channels in the microwave and submillimeter spectral regions (Racette et al. 2005), and multichannel microwave radiometer profilers (MWRP) from Radiometrics (the same company that built the operational two-channel MWRs) were deployed during the 2004 and 2007 IOPs.

The 1999 and 2004 IOPs demonstrated that the observations at 183 GHz were indeed much more sensitive to the PWV in the dry Arctic atmosphere than the 22.2-GHz observations (e.g., Racette et al. 2005; Mattioli et al. 2007), and, when combined with the 22.2-GHz observation, accurate PWV retrievals could be performed for the entire range of PWVs that exists at the NSA site. Furthermore, there was good agreement in the PWVs retrieved individually from the 22-GHz and 183-GHz radiometers in the PWV range, where both had sensitivity (i.e., from roughly 0.4 to 1.0 cm). When taken together with the fact that the strengths of

both of these water vapor absorption lines were determined the same way via measurements of the Stark effect, the program could conclude that the 183-GHz measurements were included in the Rosetta Stone conclusions (i.e., that they could serve as a PWV reference). These studies were so conclusive that DOE issued a small business innovation research (SBIR) funding opportunity to give vendors the opportunity to develop operational 183-GHz radiometers; ultimately, two different vendors would seize this opportunity and develop radiometers that would be evaluated at the NSA site during RHUBC-I in 2007. These radiometers were then evaluated side by side, together with the GSR, during RHUBC-I and were found to agree very well; Cimini et al. (2009) concluded that the ARM Program was now able to measure PWV in the Arctic to better than 3%. This significant improvement in water vapor measurements allowed Delamere et al. (2010) to further refine the modeled strength of the infrared water vapor continuum absorption model. These new 183.3-GHz radiometers are operational at the NSA site, and automated PWV and liquid water path retrievals have been developed for them (Cadeddu et al. 2009).

An additional finding of the first two WVIOPs concerned the accuracy of radiosonde humidity measurements in the Arctic. The first two WVIOPs analyzed the ARM-launched RS80-H (during the 1999 experiment) and the RS90 (during the 2004 campaign) radiosondes, as well as the VIZ/Sippican resistive hygristor radiosondes (Wade 1994) that the National Weather Service was launching twice daily approximately 5 km away from the NSA site. These comparisons demonstrated that the VIZ/Sippican moisture sensors were very poor, with wet biases in the lower troposphere and dry biases in the upper troposphere (Mattioli et al. 2007, 2008). However, the comparisons with both types of Vaisala sondes demonstrated that, as at SGP, the Vaisala sondes were able to measure the profile of the water vapor mixing ratio relatively accurately if a height-independent scale factor, such as the ratio of the PWVs from the 183-GHz radiometer and the sonde itself, was applied to the entire humidity profile (Racette et al. 2005; Mattioli et al. 2007, 2008).

## 6. Improvements to the microwave radiative transfer model

The microwave radiative transfer models used by the ARM Program have sufficient accuracy for PWV retrievals because the strengths of the relevant water vapor absorption lines are known with high accuracy, and the microwave observations were performed at the spectral location at which errors in the half-width of the absorption line have minimal impact. However, the continued development of microwave radiometer instrumentation would provide new observations that would be used by the program to continue to evaluate and improve the accuracy of the half-widths of the 22.2- and 183.3-GHz water vapor absorption lines, as well as the underlying water vapor continuum absorption model.

The first microwave radiometer with more than two channels that was operated routinely by the program was the 12-channel MWRP (Solheim et al. 1998a), which was developed in the late 1990s; the MWRP had five channels along the side of the 22.2-GHz water vapor absorption line. MWRP observations began at the SGP site in February 2000. The SBIR process also resulted in two new radiometers that made multiple observations along the 183.3-GHz line, both of which were deployed at the NSA site prior to RHUBC-I: the G-band microwave radiometer (GVR; Cadeddu et al. 2007b) and the G-band microwave radiometer profiler (GVRP; Cimini et al. 2009). Finally, the desire to have increased sensitivity to low amounts of liquid water path led to the program acquiring microwave radiometers with channels at 90 and 150 GHz (Shupe et al. 2016, chapter 19).

Line-by-line radiative transfer models like the LBLRTM require a spectroscopic database with the position, strength, width, and other properties of each absorption line for all gases that absorb radiation in Earth's atmosphere. The High-Resolution Transmission (HITRAN) database, for example, is a compilation of these parameters and has been updated many times over the decades as new laboratory and field observations, theoretical calculations, and other insights have improved our understanding of these parameters (e.g., Rothman et al. 1992, 2005). Since there are only a relatively small number of absorption lines in the microwave portion of the spectrum, microwave absorption models typically have these line parameters hardcoded, and thus the model reflects the state of the knowledge at the time the model was created.

Liljegren et al. (2005) were the first to use the new MWRP observations to evaluate and characterize the line strength and half-width of the 22.2-GHz line. They confirmed that the line strength suggested by the Stokes effect matched the MWRP observations the best but that the newly determined line width in the 2004 version of HITRAN was more accurate than the widths used in either the Rosenkranz (1998) or the Liebe and Layton (1987) models. Payne et al. (2008) used the MWRP at the SGP and the GVR at the NSA to evaluate the line widths of the 22.2- and 183.3-GHz lines and demonstrated that the line widths predicted by a new theoretical calculation matched the widths derived from the

observations to within 3%. The excellent agreement in the widths between observations and theory gave confidence to the theory, and the monochromatic radiative transfer model (MonoRTM) was modified to include both these widths and the temperature dependence of these widths that were suggested by the theory (Payne et al. 2008). These changes to the modeled widths of these spectral lines greatly improved the accuracy of humidity profiles that were retrieved from these multichannel microwave radiometers (Liljegren et al. 2005; Payne et al. 2008). The multichannel MWRP was also useful in evaluating the oxygen spectroscopy at 60 GHz (Cadeddu et al. 2007a); this spectral region is used for profiling atmospheric temperature.

These multichannel observations, together with a long-term analysis of the two-channel MWR data at the SGP site and the 150-GHz data that were collected during an ARM Mobile Facility (AMF) deployment to the Black Forest in Germany (Wulfmeyer et al. 2011), were used to make important refinements to the water vapor continuum absorption model used in the microwave. The water vapor continuum model has two components: the self-broadened component, where water vapor molecules interact with other water vapor molecules and the foreign-broadened component, where water vapor molecules interact with nitrogen and oxygen molecules (Mlawer et al. 2012). These observations, which spanned a large range of PWV as a result of the observations coming from different climatic locations, helped to more accurately separate the contributions from the two components and determine the strength of the absorption of each more accurately (Turner et al. 2009; Payne et al. 2011; Fig. 13-4), leading to improvement in the Mlawer–Tobin–Clough–Kneizys–Davies (MT_CKD) water vapor continuum model from v2.1 to v2.4. This improvement in the modeled strength of the water vapor continuum in the microwave portion of the spectrum would have a large impact on the strength of the modeled absorption by the continuum in the far-infrared (Delamere et al. 2010; Mlawer et al. 2012), which would, in turn, have a significant impact on both the radiative and dynamical evolution of global climate model simulations (Turner et al. 2012).

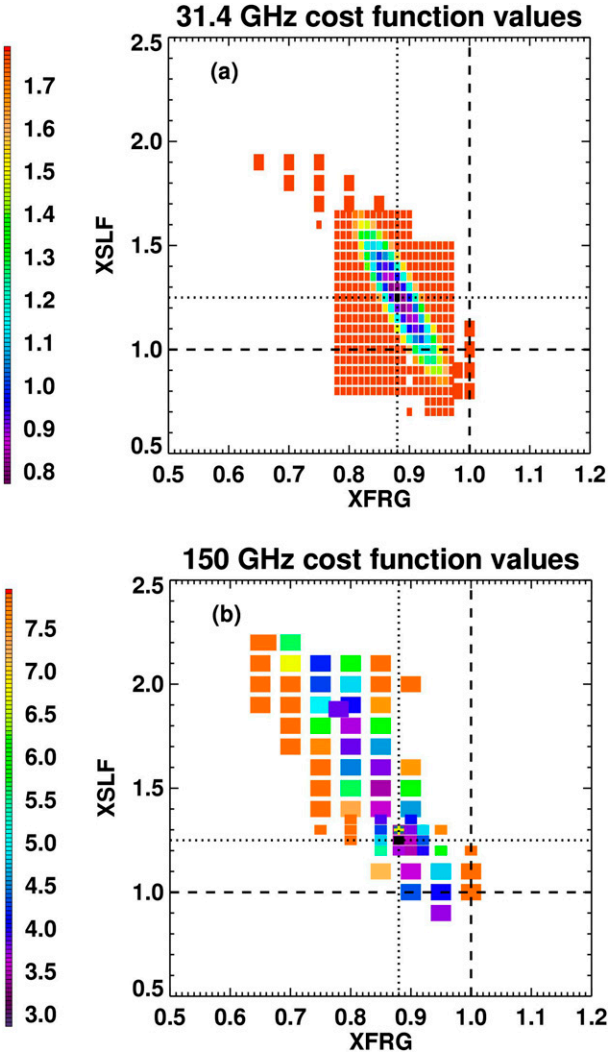


FIG. 13-4. Cost function surfaces for different scaling factors applied to the MT_CKD v2.1 self- (XSLF) and foreign- (XFGN) broadened water vapor continuum coefficients at (a) 31.4 and (b) 150 GHz. The purple regions indicate better fits of the coefficients to the two datasets (31.4 and 150 GHz, respectively). Crosshairs with dashed lines show the positions of the v2.1 values, while crosshairs with dotted lines show the new values of the water continuum that were incorporated into MT_CKD v2.4, which were values that gave the best results at the two frequencies simultaneously. Modified from Payne et al. (2011).

## 7. Other technologies

A wide range of other water vapor technologies played an important role during the early ARM years and were part of the WVIOPs. These technologies included the Raman lidar, global positioning system (GPS) PWV estimates, and solar attenuation measurements of PWV. The development of the ARM Raman lidar is a colorful story and one of the many successes of the ARM Program; a full discussion is provided by Turner et al. (2016, chapter 18). The GPS and solar attenuation methods provided a relatively affordable way to measure PWV routinely at many sites, such as the SGP extended facilities, and thereby provide a measure of the spatial variability of the water vapor field over the large SGP domain. Furthermore, several different retrieval algorithms were developed to provide thermodynamic profiles from remote sensors at the ARM sites; these profiles would have coarser vertical resolution but

much higher temporal resolution than radiosondes. Finally, different analysis approaches were suggested on how to merge these different datasets together to provide humidity profiles throughout the troposphere over the diurnal cycle by blending together different instruments.

### *a. GPS PWV observations*

The GPS sensor measures the propagation delay that occurs as the signal emitted by an orbiting satellite reaches the receiver on the ground. This delay, after accounting for the frequency-dependent delay caused by the ionosphere, is the result of the refractivity of the (primarily) lower troposphere, and the total delay is often separated into hydrostatic (sometimes called the dry) and wet components. The GPS measurement is usually accompanied by a measure of atmospheric pressure at the surface; this observation allows the hydrostatic component of the delay to be accurately estimated. The wet delay, which is the sum of the delay from both water vapor and liquid water, is computed as the residual between the total observed delay and the computed dry delay. However, the wet delay is dominated by water vapor in most conditions because of the difference in the mass of water vapor relative to the mass of liquid water in a column of air. Thus, the computed hydrostatic delay (from the surface pressure measurement), together with the GPS-observed delays, can be translated into a measure of PWV along the slant path to the satellite (i.e., SPWV) using a wet delay ''mapping function,'' which is essentially a characteristic water vapor profile that can be scaled (Niell 1996; Niell et al. 2001). Since the GPS sensor is able to track multiple satellites simultaneously, many different SPWV values can be derived, and these are typically processed to provide one PWV estimate over the GPS sensor every 30 min.

The technique to derive PWVs from GPS observations was first described by Bevis et al. (1992), demonstrated in the GPS/STORM experiment in the spring of 1993, and integrated at the ARM SGP site shortly thereafter (Gutman et al. 1994). The technology was very exciting, as GPS sensors were much more affordable than MWRs and thus could be deployed en masse to form a PWV observation network. Thus, many different groups performed comparisons between sondes, MWRs, solar radiometers, and GPS PWV observations (e.g., Liljegren and Lesht 1996; Wolfe and Gutman 2000; Braun et al. 2001; Liou et al. 2001; Braun et al. 2003; Mattioli et al. 2005; Champollion et al. 2009; Alexandrov et al. 2009). The ARM Program played a significant role advancing the science behind the GPS PWV measurements, both in improving the accuracy of the algorithms and in using these retrievals to advance our understanding of atmospheric water vapor.

As with all retrieval algorithms, there were multiple ways to derive the PWV from the GPS observations, and hence different software analysis tools were developed, such as GPS Analysis at Massachusetts Institute of Technology (GAMIT; King and Bock 1996) and Bernese (Rothacher 1992). These software packages are essentially forward models, and each makes somewhat different assumptions and approximations. In particular, there were two important decisions that needed to be made and were debated by the GPS analysis community. The first decision concerned the lowest cutoff angle that should be used in the analysis: i.e., what is the lowest elevation of the GPS satellite above the horizon that should be allowed to contribute to the solution? The GPS signal-to-noise ratio is very small (i.e., less than 1), and thus collecting data at lower-elevation angles when the satellite is near the horizon increases the contribution to the wet delay (and hence the signal-to-noise) because the atmospheric pathlength is longer, and the water vapor concentration is the highest in the boundary layer. However, the propagating GPS signal could multipath (i.e., reflect off the ground) when the satellite was close to the horizon, which would result in overestimates of the wet delay and hence SPWV because of inappropriately long pathlengths. Ultimately, through long-term comparisons at the SGP site and WVIOP results, the compromise between good sensitivity to boundary layer moisture and minimal multipath errors suggested that a 7° elevation angle was the best cutoff angle to use (Fang et al. 1998). The second decision facing the GPS community was the choice of mapping function, as different mapping functions became more important for lower-elevation angles especially below 5°. Different mapping functions could result in changes of up to several percent in PWV, and the impact of the mapping function depended heavily on the cutoff angle used. (Thus, the cutoff angle decision helped largely to mitigate this source of uncertainty.) Furthermore, WVIOPs and long-term analysis at the ARM site with the MWRs demonstrated that using a single mapping function for both day and night processing often resulted in small seasonal and diurnal biases in the derived PWV (Rocken et al. 2001). The focus offered by the WVIOPs (and other experiments) provided opportunities to directly compare GPS processing algorithms and choices, which ultimately led to a convergence between the different algorithms (Revercomb et al. 2003).

One of the possible applications of a dense network of GPS sensors was to derive profiles of water vapor from the SPWV observations using tomographic retrieval techniques. Many GPS sensors were installed around the SGP domain, thus providing the opportunity to

perform the tomographic retrieval and to compare the results with independent water vapor profiles observed by instruments at the SGP Central Facility. Champollion et al. (2009) did exactly this and demonstrated that the GPS-derived water vapor field, while smoother in height than that observed by other instruments, had sufficient accuracy to provide useful spatial information during a rapidly changing water vapor field. This helped improve our understanding of the evolution of the boundary layer during a convective initiation event. That said, it has become the practice of the operational numerical modeling community to directly assimilate the observed GPS tropospheric delays instead of the SPWV values or the tomographic reconstructions (Smith et al. 2007).

### b. *Solar PWV observations*

Solar attenuation methods offer a different way to derive PWV. These techniques usually make use of direct-beam measurements of solar irradiance in a spectrally narrow (order 5–10 nm wide) water vapor absorption band; the most typically used band is centered at 940 nm. The accuracy of the PWV retrievals from these methods depends strongly on the instrument calibration, the characterization of the instrument parameters (e.g., the bandpass of the instrument), and the accuracy of the radiative transfer model used in the retrieval. The WVIOPs provided excellent opportunities to bring additional solar radiometers to the SGP site and evaluate the different retrieval methods to get PWVs from these observations. However, since the solar technique measures the absorption of radiation in water vapor spectral bands, the presence of clouds and optically thick aerosol layers that extinguish the solar radiation in these bands hampers these retrievals.

Another instrument that matured with ARM funding was the multifilter rotating shadowband radiometer (MFRSR; Harrison et al. 1994). The MFRSR was deployed at many of the ARM sites and, in particular, was deployed at both the Central and extended facilities at the SGP site. Michalsky et al. (1995) derived a method to derive total column PWV along the slant path (i.e., SPWV toward the sun) from the MFRSR observations, which could be converted to PWV by assuming that the water vapor field was horizontally homogeneous. Halthore et al. (1997) and Kiedron et al. (2003) also developed algorithms to retrieve PWV from 940-nm solar observations.

During the 1997 WVIOP, other narrowband solar radiometers were brought to the SGP site, including the six-channel Ames airborne tracking sunphotometer (AATS-6; Schmid et al. 2001), the Cimel sunphotometer (Holben et al. 1998), and the rotating shadowband spectrometer (RSS; Harrison et al. 1999). PWV retrievals from these three radiometers and the MFRSR were compared to the MWR. Initially, good results were obtained from all four solar radiometers and the MWR; however, a deeper analysis suggested that there were compensating errors that were affecting the comparison (Schmid et al. 2001). For example, the various retrieval techniques used different radiative transfer models to derive PWV from the solar observations. When the same radiative transfer model was used for all retrievals, the spread in the PWV results among the solar radiometers increased (Schmid et al. 2001). Furthermore, Giver et al. (2000) found an error in the absorption line information for the 940-nm water vapor band in the HITRAN database used by the radiative transfer models, and using the updated line information resulted in the PWV derived from the solar radiometers being 6%–14% drier than the MWR-retrieved value (Schmid et al. 2001). These 6%–14% differences were thought to be related to uncertainties associated with instrument calibration and incomplete knowledge of the spectral bandpass (MFRSR and AATS-6) or slit-function (RSS) profiles, although uncertainties in either the water vapor spectroscopy and/or the water vapor continuum absorption model in the near-infrared were also candidates.

An updated analysis was performed by Alexandrov et al. (2009) using long-term MFRSR and MWR data at the SGP site, together with Cimel and AATS-6 radiometer data collected at the SGP during the 2000 WVIOP. This new comparison used the updated spectroscopy that was available in the HITRAN 2004 database. This study demonstrated that the agreement among the PWVs retrieved from the solar radiometers was within 4% but that again the solar radiometer retrievals were about 10% drier than the MWR-retrieved PWV, with the difference being larger when the PWV was more than 2 cm (Alexandrov et al. 2009). Like Schmid et al. (2001), the Alexandrov et al. (2009) study concluded that the differences are likely not caused by the radiometric calibration of the solar radiometers, but are more likely due to spectroscopy or errors in the spectral bandpass of the solar radiometers.

### c. *Ground-based thermodynamic profile retrievals*

The original plan of the ARM Program was for limited use of radiosondes, with remote sensors providing the routine water vapor profiles required by the program. Furthermore, the remote sensors would provide higher-time-resolution profiles of water vapor than are possible with radiosondes, which would be useful in characterizing the temporal evolution of the moisture in the boundary layer as atmospheric fronts and other disturbances passed overhead. It was hoped that the

Raman lidar would provide these observations at the SGP site, but given the expense of this system, only a single Raman lidar would be deployed by the program at the SGP site.[2] Thus, other remote sensors would have to provide the higher-temporal-resolution observations at the other ARM sites.

Spectrally resolved radiance observations from passive microwave and infrared radiometers have been used to profile the troposphere from space since the 1970s. The original microwave profiling (MWRprof) algorithm was developed by Ed Westwater and colleagues, using the two-channel MWR data together with the temperature profiles from the radar wind profiler/RASS to get profiles of temperature and humidity in the boundary layer (Han and Westwater 1995; Stankov et al. 1996; Westwater 1997). It provided very low-vertical-resolution profiles of humidity because of the limited spectral information available to the retrieval. Nonetheless, this algorithm was one of the earliest value-added products implemented within the ARM Data Management Facility (McCord and Voyles 2016, chapter 11). The development of the MWRP provided additional spectral information for the microwave retrieval community, and newer and more advanced algorithms were developed (e.g., Solheim et al. 1998b; Ware et al. 2003; Liljegren et al. 2005). The MWRP and radiometers like it are able to provide low-vertical-resolution but high-temporal-resolution temperature and humidity profiles in most weather situations aside from medium-to-heavy precipitation and thus are well suited for operational networks like ARM (e.g., Hardesty and Hoff 2012). Similar retrieval algorithms also were developed for the multifrequency observations from the GVR and GVRP (e.g., Racette et al. 2005; Cimini et al. 2010). In addition, since clouds are usually optically thin at microwave frequencies, profiles of temperature and humidity can be retrieved from MWRP observations at and above the cloud height, wherein other methods, such as the Raman lidar, are largely limited to altitudes below cloud base.

In the mid-1990s, Bill Smith and Wayne Feltz developed a retrieval algorithm that used infrared radiance data observed by the AERI to get profiles of temperature and humidity (AERIprof; Feltz et al. 1998; Smith et al. 1999). These AERIprof retrievals were used to characterize frontal passages and drylines over the SGP (e.g., Feltz et al. 1998; Turner et al. 2000). The ARM Program deployed five AERI systems over the SGP domain from 1998 to 2003, and the thermodynamic retrieval data from this network were used to evaluate the water vapor and temperature evolution and convective stability indices during tornadic and nontornadic storms (Feltz and Mecikalski 2002; Wagner et al. 2008). The AERI thermodynamic retrievals are also used as part of the Raman lidar processing algorithms (Turner et al. 2002) and for providing input to other retrieval algorithms, such as the cumulus entrainment algorithm of Wagner et al. (2013). Löhnert et al. (2009) demonstrated that the information content in the AERI observations was 2–4 times higher than the MWRP for both temperature and water vapor, but the Smith–Feltz AERI algorithm was limited to cases where there are no clouds in the AERI field of view. However, recent developments have demonstrated the ability to retrieve thermodynamic properties from the AERI under clouds (Turner and Löhnert 2014).

### *d. Merging water vapor datasets together*

The ultimate goal of the program with respect to water vapor (and temperature) fields is to specify these properties at all times and heights above its facilities. This type of data product is needed for a wide range of research topics that are important to the ARM Program. With no single instrument able to provide these profiles in all weather conditions at high temporal [$O(10)$ min] and vertical resolution, this data product must result from a combination of observations from several sensors and perhaps output from numerical models.

Research on how to best marry together observations from different remote sensors began in earnest in the program long before the remote sensors themselves were mature. For example, Stankov et al. (1996) presented different ways to integrate data from remote sensors, such as MWRs, wind profilers, and more. Han et al. (1997) used a Kalman filter to merge water vapor data from the MWR and (NASA) Raman lidar in order to provide profiles where the Raman lidar observations were either limited by clouds or by solar noise (the latter during the daytime).

ARM has developed a simple "merged sonde" data product called MERGESONDE to provide the baseline thermodynamic profiles at all times and heights above the ARM sites that are needed to compute radiative heating rates in clear and cloudy atmospheres (McFarlane et al. 2016, chapter 20). This algorithm combines radiosonde, MWR, surface meteorological data, and numerical weather prediction model output to derive these thermodynamic fields. However, this product is relatively simple and currently does not include any of the measurements or retrievals

[2] The success of the SGP Raman lidar, together with the funding received in 2009 from the American Recovery and Reinvestment Act (ARRA), allowed the program to construct a nearly identical Raman lidar and deploy it to the Darwin TWP site in late 2010. The program recently constructed a third Raman lidar that was deployed at the new ARM site in Oliktok Point, Alaska, in 2014.

from the Raman lidar, AERI, or profiling MWRs, although upgrades are planned for future versions.

Tobin et al. (2006) have developed a merged thermodynamic product that combines radiosondes, AERIprof retrievals, and MWR PWV observations to derive a best-estimate temperature and water vapor profile for validating similar products from NASA and EUMETSAT satellites [e.g., products derived from the Atmospheric Infrared Sounder (AIRS), Infrared Atmospheric Sounding Interferometer (IASI), and Cross-Track Infrared Sounder (CrIS) sensors]. The ARM Program, in collaboration with NASA and in the spirit of being a user facility (Ackerman et al. 2016, chapter 3), has conducted several dedicated multimonth IOPs at the SGP, NSA, and Tropical Western Pacific (TWP) sites to support these satellite-validation IOPs; these IOPs have been extremely useful in continually improving the operational data products derived from these satellites (e.g., Tobin et al. 2006; Bedka et al. 2010).

One of the most important value-added products in the ARM Program is the variational analysis product that was developed by Minghua Zhang and colleagues. This algorithm takes observational data from a large number of sensors (e.g., surface meteorological stations, MWRs, radiosondes, and more) and merges them together to create a dataset that can be used to drive single-column and cloud-resolving models (Zhang and Lin 1997; Zhang et al. 2001, 2016, chapter 24).

## 8. Current status and future outlook

Improving water vapor measurements was an extremely high priority in the first decade of the ARM Program. A large number of investigators worked on developing, characterizing, and improving different technologies as part of this effort. Many different instruments matured into operational instruments as a result of this funding: the MWR, AERI, Raman lidar, GPS, and GVR/GVRP.

Several WVIOPs were organized at the SGP and NSA sites to provide opportunities to bring together these investigators, along with additional research-grade instruments, to evaluate the ARM operational and research-grade instruments. The results from these IOPs, along with the longer-term comparisons of the operational ARM instruments, greatly improved our understanding of these instruments, including details in calibration, the underlying radiative transfer models, and sensitivity and precision of the observations themselves. Ultimately, these efforts reduced the uncertainty in the profile of the water vapor mixing ratio in the lower-to-middle troposphere from 15%–20% in the early days of the ARM Program to approximately 3% in both the SGP and NSA regions—a remarkable improvement. This new level of accuracy in the water vapor measurement opened the door to making important improvements in the absorption spectroscopy in microwave, infrared, and near-infrared radiative transfer models (Mlawer and Turner 2016, chapter 14).

This large improvement in the program's ability to measure the water vapor profile accurately, which was achieved largely in the late 1990s for midlatitude sites, allowed the program managers to reprioritize how the program was utilizing its research funds. Thus, starting around 2002, there was a decrease in the number of investigators working on profiling water vapor so that additional investigators could be funded to support other ARM programmatic objectives (Mather et al. 2016, chapter 4).

There is more work that can be done. The accuracy of the water vapor spectroscopy in the visible and near-infrared is still uncertain; this is quite possibly the reason why the solar PWV retrievals that use the 940-nm water vapor absorption band do not agree with the MWR's PWV retrievals. Another area that needs work concerns water vapor measurements in the upper troposphere. There has been some work to evaluate the accuracy of water vapor observations in this region (e.g., Ferrare et al. 2004; Soden et al. 2004; Miloshevich et al. 2006), but additional work (especially in the Arctic and tropical atmospheres) is needed. Accurate upper-tropospheric water vapor observations are very important to understand processes at work in the upper troposphere, such as ice nucleation mechanisms (e.g., Comstock et al. 2004) and radiative processes that control outgoing infrared emission to space (e.g., Ferrare et al. 2004).

Finally, the program needs to develop improved data synthesis products to create water vapor datasets to better cover all heights and times above the ARM sites and to provide some spatial context (e.g., for gradients and smaller-scale inhomogeneities) around the sites. These improvements will require utilizing the remote sensors at the sites, any sensors that are distributed around the sites (e.g., surface meteorological observations, MFRSRs, and GPS), and satellite observations. Tomographic techniques that utilize slant path observations from a large number of sensors also may contribute to this challenge. The deployment of Raman lidars at several of the ARM sites will help address some of this need, as well as the efforts currently underway to get the AERIprof retrieval algorithm (or its successor, which is able to work in cloudy scenes) ported to the tropics and Arctic. However, it will be very important that these merged products are well characterized and have quantified uncertainty estimates so that the scientific community can use these data products properly.

While there is much that still remains, the program has made tremendous strides in its ability to measure water vapor. The improvements in this area are certainly among the highlights of the first 20 years of the ARM Program.

## APPENDIX

### The AERI

Accurate spectrally resolved downwelling infrared radiance measurements were required to address the problems raised by ICRCCM (Ellingson et al. 2016, chapter 1; Ellingson and Fouquart 1991). The AERI was developed under the auspices of the ARM Instrument Development Program (Stokes 2016, chapter 2) to provide these observations. The AERI traces its origins back to both the ICRCCM requirement and to the desire to retrieve thermodynamic profiles from space using passive spectral infrared measurements. The AERI is one of the observational success stories of ARM and would play a key role in characterizing the accuracy of water vapor measurements made by the ARM Program (Turner et al. 2003b), improving the accuracy of the LBLRTM (Tobin et al. 1999; Turner et al. 2004; Delamere et al. 2010; Mlawer et al. 2012), and serving as input to cloud and aerosol retrieval algorithms (e.g., Mace et al. 1998; Comstock et al. 2007; Turner 2008).

The AERI was designed and fabricated by the Space Science and Engineering Center (SSEC) at the University of Wisconsin–Madison (Knuteson et al. 2004a,b). SSEC has a long history in developing satellite observation systems and using these data to characterize clouds and thermodynamic profiles in the atmosphere (e.g., Suomi and Vonder Haar 1969; Vonder Haar and Suomi 1971; Smith et al. 1981). SSEC developed an airborne infrared interferometer called the High-Resolution Infrared Sounder (HIS) in the mid-1980s to demonstrate the improved vertical resolution of retrieved temperature and humidity profiles that could be achieved if a satellite sensor had the high spectral resolution of an interferometer (Revercomb et al. 1988). In a proof-of-concept experiment, SSEC operated the HIS in an uplooking mode during the Ground-Based Atmospheric Profiling Experiment (GAPEX; Smith et al. 1990). The success of GAPEX led to the development of the first dedicated ground-based interferometer by SSEC, which was called the ground-based HIS (GB-HIS). The GB-HIS demonstrated the feasibility of the instrument design and calibration approach (Knuteson et al. 2004a). SSEC learned many lessons from the development and operation of the GB-HIS; these lessons and ARM funding led to the development of the prototype AERI system (called AERI-00).

The AERI-00 was first deployed in the SPECTRE field campaign (Ellingson and Wiscombe 1996; Ellingson et al. 2016, chapter 1). Based upon the results from this experiment, a set of instrument specifications was developed for the ARM Program. Principal among these requirements was the need for the instrument to work operationally without manual intervention. The detectors of these interferometers are cooled cryogenically to get the required signal-to-noise ratio. Early versions of these interferometers used liquid nitrogen to cool the detectors, which required manual refilling every 8 or 24 h. SSEC developed the first truly operational AERI (called the AERI-01) with ARM support; this system used a mechanical Sterling cooler to keep the detectors cold (Knuteson et al. 2004a). The AERI-01 was first deployed to the SGP site in the summer of 1995, replacing the AERI-00 that had been operating there since 1992. Continued experience with the AERI-01 led to improvements in the AERI technology that were incorporated into the AERI-v2 systems that were subsequently deployed at all of the primary ARM sites (e.g., SGP, NSA, TWP, and AMF). In the meantime, the AERI-01 has continued to operate at the SGP site for nearly 20 years, allowing the first long-term evaluation of spectral downwelling IR radiation to be performed (Gero and Turner 2011).

The strength of the AERI is its calibration. The use of two well-characterized (in both temperature and emissivity) blackbodies, together with the quantification of the nonlinear behavior of the detector, results in a radiometric calibration accuracy of better than 1% of the ambient radiance ($3\sigma$) (Knuteson et al. 2004b). The instrument also performs a spectral calibration and corrects for self-apodization artifacts that result from the finite field of view (Knuteson et al. 2004b), which makes it significantly easier to compare the AERI-observed radiances to those computed with a line-by-line model (e.g., Turner et al. 2004; Delamere et al. 2010) or to use them in a thermodynamic profiling retrieval algorithm (e.g., Feltz et al. 1998, 2003; Turner and Löhnert 2014).

The original temporal resolution of the AERI was set to 10 min; this was a compromise between achieving a good signal-to-noise ratio in the observed radiance for spectroscopic validation and profiling while maintaining the temporal resolution needed to resolve evolving atmospheric conditions. However, the AERI radiance observations soon were being used in retrieval algorithms to characterize cloud properties (e.g., Mace et al. 1998; Deslover et al. 1999; Turner et al. 2003a), which can change very rapidly as the cloud advects over the

instrument. Thus, the program changed the temporal sampling strategy of the AERI so that a radiance spectrum was collected every 20–30 s, and a principal component-based noise filter was used to reduce the increased random error back to approximately the same noise level that was inherent in the 10-min data (Turner et al. 2006).

## REFERENCES


Ackerman, T. P., T. S. Cress, W. R. Ferrell, J. H. Mather, and D. D. Turner, 2016: The programmatic maturation of the ARM Program. *The Atmospheric Radiation Measurement (ARM) Program: The First 20 Years, Meteor. Monogr.*, No. 57, Amer. Meteor. Soc., doi:10.1175/AMSMONOGRAPHS-D-15-0054.1.

Alexandrov, M. D., and Coauthors, 2009: Columnar water vapor retrievals from multifilter rotating shadowband radiometer data. *J. Geophys. Res.*, **114**, D02306, doi:10.1029/2008JD010543.

ARM, 2016: Appendix A: Executive summary: Atmospheric Radiation Measurement Program Plan. *The Atmospheric Radiation Measurement (ARM) Program: The First 20 Years, Meteor. Monogr.*, No. 57, Amer. Meteor. Soc., doi:10.1175/AMSMONOGRAPHS-D-15-0036.1.

Bedka, S., R. O. Knuteson, H. E. Revercomb, D. C. Tobin, and D. D. Turner, 2010: An assessment of the absolute accuracy of the Atmospheric Infrared Sounder v5 precipitable water vapor product at tropical, midlatitude, and Arctic ground-truth sites: September 2002 through August 2008. *J. Geophys. Res.*, **115**, D17310, doi:10.1029/2009JD013139.

Bevis, M., S. Businger, T. A. Herring, R. A. Anthes, C. Rocken, and R. H. Ware, 1992: GPS meteorology: Remote sensing of atmospheric water vapor using the global positioning system. *J. Geophys. Res.*, **97**, 15 787–15 801, doi:10.1029/92JD01517.

Braun, J., C. Rocken, and R. Ware, 2001: Validation of line-of-sight water vapor measurements with GPS. *Radio Sci.*, **36**, 459–472, doi:10.1029/2000RS002353.

——, ——, and J. Liljegren, 2003: Comparisons of line-of-sight water vapor observations using the global positioning system and a pointing microwave radiometer. *J. Atmos. Oceanic Technol.*, **20**, 606–612, doi:10.1175/1520-0426(2003)20<606:COLOSW>2.0.CO;2.

Cadeddu, M. P., S. A. Clough, V. H. Payne, K. Cady-Pereira, and J. C. Liljegren, 2007a: Effect of the oxygen line-parameter modeling on temperature and humidity retrievals from ground-based microwave radiometers. *IEEE Trans. Geosci. Remote Sens.*, **45**, 2216–2223, doi:10.1109/TGRS.2007.894063.

——, J. C. Liljegren, and A. Pazmany, 2007b: Measurements and retrievals from a new 183-GHz water-vapor radiometer in the Arctic. *IEEE Trans. Geosci. Remote Sens.*, **45**, 2217–2223, doi:10.1109/TGRS.2006.888970.

——, D. D. Turner, and J. C. Liljegren, 2009: A neural network for real-time retrievals of PWV and LWP from Arctic millimeter-wave ground-based observations. *IEEE Trans. Geosci. Remote Sens.*, **47**, 1887–1900, doi:10.1109/TGRS.2009.2013205.

Cady-Pereira, K., M. W. Shephard, D. D. Turner, E. J. Mlawer, S. A. Clough, and T. J. Wagner, 2008: Improved daytime column-integrated precipitable water vapor from Vaisala radiosonde humidity sensors. *J. Atmos. Oceanic Technol.*, **25**, 873–883, doi:10.1175/2007JTECHA1027.1.

Champollion, C., C. Flamant, O. Bock, F. Masson, D. D. Turner, and T. Weckwerth, 2009: Mesoscale GPS tomography applied to the 12 June 2002 convective initiation event of IHOP_2002. *Quart. J. Roy. Meteor. Soc.*, **135**, 645–662, doi:10.1002/qj.386.

Cimini, D., E. R. Westwater, A. J. Gasiewski, M. Klein, V. Leuski, and S. Dowlatshahi, 2007: The Ground-Based Scanning Radiometer (GSR): A powerful tool for the study of the Arctic atmosphere. *IEEE Trans. Geosci. Remote Sens.*, **45**, 2759–2777, doi:10.1109/TGRS.2007.897423.

——, F. Nasir, E. R. Westwater, V. H. Payne, D. D. Turner, E. J. Mlawer, M. L. Exner, and M. Cadeddu, 2009: Comparison of ground-based millimeter-wave observations in the Arctic winter. *IEEE Trans. Geosci. Remote Sens.*, **47**, 3098–3106, doi:10.1109/TGRS.2009.2020743.

——, E. R. Westwater, and A. J. Gasiewski, 2010: Temperature and humidity profiling in the Arctic using ground-based millimeter-wave radiometry and 1DVAR. *IEEE Trans. Geosci. Remote Sens.*, **48**, 1381–1388, doi:10.1109/TGRS.2009.2030500.

Clough, S. A., Y. Beers, G. P. Klein, and L. S. Rothman, 1973: Dipole moment of water vapor from Stark measurements of $H_2O$, HDO, and $D_2O$. *J. Chem. Phys.*, **59**, 2254–2259, doi:10.1063/1.1680328.

——, M. J. Iacono, and J.-L. Moncet, 1992: Line-by-line calculation of atmospheric fluxes and cooling rates: Application to water vapor. *J. Geophys. Res.*, **97**, 15 761–15 781, doi:10.1029/92JD01419.

——, M. W. Shephard, E. J. Mlawer, J. S. Delamere, M. J. Iacono, K. Cady-Pereira, S. Boukabara, and P. D. Brown, 2005: Atmospheric radiative transfer modeling: A summary of the AER codes. *J. Quant. Spectrosc. Radiat. Transfer*, **91**, 233–244, doi:10.1016/j.jqsrt.2004.05.058.

Comstock, J. M., T. P. Ackerman, and D. D. Turner, 2004: Evidence of high ice supersaturation in cirrus clouds using ARM Raman lidar measurements. *Geophys. Res. Lett.*, **31**, L11106, doi:10.1029/2004GL019705.

——, and Coauthors, 2007: An intercomparison of microphysical retrieval for upper-tropospheric ice clouds. *Bull. Amer. Meteor. Soc.*, **88**, 191–204, doi:10.1175/BAMS-88-2-191.

Delamere, J. S., S. A. Clough, V. Payne, E. J. Mlawer, D. D. Turner, and R. Gamache, 2010: A far-infrared radiative closure study in the Arctic: Application to water vapor. *J. Geophys. Res.*, **115**, D17106, doi:10.1029/2009JD012968.

Deslover, D. H., W. L. Smith, P. K. Piironen, and E. W. Eloranta, 1999: A methodology for measuring cirrus cloud visible-to-infrared spectral optical depth ratios. *J. Atmos. Oceanic Technol.*, **16**, 251–262, doi:10.1175/1520-0426(1999)016<0251:AMFMCC>2.0.CO;2.

DOE, 1990: Atmospheric Radiation Measurement Program Plan. DOE Tech. Doc. DOE/ER-0441, 121 pp. [Available online at https://www.arm.gov/publications/doe-er-0441.pdf.]

Ellingson, R. G., and Y. Fouquart, 1991: The intercomparison of radiation codes in climate models: An overview. *J. Geophys. Res.*, **96**, 8925–8927, doi:10.1029/90JD01618.

——, and W. J. Wiscombe, 1996: The Spectral Radiance Experiment (SPECTRE): Project description and sample results. *Bull. Amer. Meteor. Soc.*, **77**, 1967–1985, doi:10.1175/1520-0477(1996)077<1967:TSREPD>2.0.CO;2.

——, R. D. Cess, and G. L. Potter, 2016: The Atmospheric Radiation Measurement Program: Prelude. *The Atmospheric Radiation Measurement (ARM) Program: The First 20 Years, Meteor. Monogr.*, No. 57, Amer. Meteor. Soc., doi:10.1175/AMSMONOGRAPHS-D-15-0029.1.

Fang, P., M. Bevis, Y. Bock, S. Gutman, and D. Wolfe, 1998: GPS meteorology: Reducing systematic errors in geodetic estimates for zenith delay. *Geophys. Res. Lett.*, **25**, 3583–3586, doi:10.1029/98GL02755.

Feltz, W. F., and J. R. Mecikalski, 2002: Monitoring high-temporal-resolution convective stability indices using the ground-based Atmospheric Emitted Radiance Interferometer (AERI) during the 3 May 1999 Oklahoma–Kansas tornado outbreak. *Wea. Forecasting*, **17**, 445–455, doi:10.1175/1520-0434(2002)017<0445:MHTRCS>2.0.CO;2.

——, W. L. Smith, R. O. Knuteson, H. E. Revercomb, H. M. Woolf, and H. B. Howell, 1998: Meteorological applications of temperature and water vapor retrievals from the ground-based Atmospheric Emitted Radiance Interferometer (AERI). *J. Appl. Meteor.*, **37**, 857–875, doi:10.1175/1520-0450(1998)037<0857:MAOTAW>2.0.CO;2.

——, ——, H. B. Howell, R. O. Knuteson, H. Woolf, and H. E. Revercomb, 2003: Near-continuous profiling of temperature, moisture, and atmospheric stability using the Atmospheric Emitted Radiance Interferometer (AERI). *J. Appl. Meteor.*, **42**, 584–597, doi:10.1175/1520-0450(2003)042<0584:NPOTMA>2.0.CO;2.

Ferrare, R. A., S. H. Melfi, D. N. Whiteman, K. D. Evans, F. J. Schmidlin, and D. Starr, 1995: A comparison of water vapor measurements made by Raman lidar and radiosondes. *J. Atmos. Oceanic Technol.*, **12**, 1177–1195, doi:10.1175/1520-0426(1995)012<1177:ACOWVM>2.0.CO;2.

——, and Coauthors, 2004: Characterization of upper-tropospheric water vapor measurements during AFWEX using LASE. *J. Atmos. Oceanic Technol.*, **21**, 1790–1808, doi:10.1175/JTECH-1652.1.

Gero, P. J., and D. D. Turner, 2011: Long-term trends in downwelling spectral infrared radiance over the U.S. Southern Great Plains. *J. Climate*, **24**, 4831–4843, doi:10.1175/2011JCLI4210.1.

Giver, L. P., C. Chackerian Jr., and P. Varanasi, 2000: Visible and near-infrared $H_2^{16}O$ line intensity corrections for HITRAN-96. *J. Quant. Spectrosc. Radiat. Transfer*, **66**, 101–105, doi:10.1016/S0022-4073(99)00223-X.

Gutman, S. I., R. B. Chadwick, D. W. Wolf, A. Simon, T. Van Hove, and C. Rocken, 1994: Toward an operational water vapor remote sensing system using the global positioning system. *Proc. Fourth Atmospheric Radiation Measurement (ARM) Science Team Meeting*, Charleston, SC, U.S. DOE, 173–180. [Available online at http://www.arm.gov/publications/proceedings/conf04/extended_abs/gutman_si.pdf?id=29.]

Halthore, R. N., T. F. Eck, B. N. Holben, and B. L. Markham, 1997: Sun photometric measurements of atmospheric water vapor column abundance in the 940-nm band. *J. Geophys. Res.*, **102**, 4343–4352, doi:10.1029/96JD03247.

Han, Y., and E. R. Westwater, 1995: Remote sensing of tropospheric water vapor and cloud liquid water by integrated ground-based sensors. *J. Atmos. Oceanic Technol.*, **12**, 1050–1059, doi:10.1175/1520-0426(1995)012<1050:RSOTWV>2.0.CO;2.

——, and ——, 2000: Analysis and improvement of tipping calibration for ground-based microwave radiometers. *IEEE Trans. Geosci. Remote Sens.*, **38**, 43–52, doi:10.1109/36.843018.

——, ——, and R. A. Ferrare, 1997: Applications of Kalman filtering to derive water vapor profiles from Raman lidar and microwave radiometers. *J. Atmos. Oceanic Technol.*, **14**, 480–487, doi:10.1175/1520-0426(1997)014<0480:AOKFTD>2.0.CO;2.

Hardesty, R. M., and R. Hoff, 2012: Thermodynamic Profiling Technologies Workshop report to the National Science Foundation and the National Weather Service. NCAR Tech. Note NCAR/TN-448+STR, 80 pp, doi:10.5065/D6SQ8XCF.

Harrison, L., J. Michalsky, and J. Berndt, 1994: Automated multifilter rotating shadow-band radiometer: An instrument for optical depth and radiation measurements. *Appl. Opt.*, **33**, 5118–5125, doi:10.1364/AO.33.005118.

——, M. Beauharnois, J. Berndt, P. Kiedron, J. Michalsky, and Q. Min, 1999: The rotating shadowband spectroradiometer (RSS) at SGP. *Geophys. Res. Lett.*, **26**, 1715–1718, doi:10.1029/1999GL900328.

Holben, B. N., and Coauthors, 1998: AERONET—A federated instrument network and data archive for aerosol characterization. *Remote Sens. Environ.*, **66**, 1–16, doi:10.1016/S0034-4257(98)00031-5.

Kiedron, P., J. Berndt, J. Michalsky, and L. Harrison, 2003: Column water vapor from diffuse irradiance. *Geophys. Res. Lett.*, **30**, 1565, doi:10.1029/2003GL016874.

King, R. W., and Y. Bock, 1996: Documentation for the GAMIT GPS analysis software, version 9.4. Massachusetts Institute of Technology and Scripps Institution of Oceanography Tech. Note, 192 pp.

Knuteson, R. O., and Coauthors, 2004a: Atmospheric Emitted Radiance Interferometer. Part I: Instrument design. *J. Atmos. Oceanic Technol.*, **21**, 1763–1776, doi:10.1175/JTECH-1662.1.

——, and Coauthors, 2004b: Atmospheric Emitted Radiance Interferometer. Part II: Instrument performance. *J. Atmos. Oceanic Technol.*, **21**, 1777–1789, doi:10.1175/JTECH-1663.1.

Liebe, H. J., and D. H. Layton, 1987: Millimeter-wave properties of the atmosphere: Laboratory studies and propagation modeling. National Telecommunications and Information Administration Tech. Rep. 87-224, 74 pp. [Available online at http://www.its.bldrdoc.gov/publications/tr-87-224.aspx.]

Liljegren, J. C., 1994: Two-channel microwave radiometer for observations of total column precipitable water vapor and cloud liquid water path. *Proc. Fifth Symposium on Global Change Studies*, Nashville, TN, Amer. Meteor. Soc., 262–269.

——, 2000: Automatic self-calibration of ARM microwave radiometers. *Microwave Radiometry and Remote Sensing of the Earth's Surface and Atmosphere*, P. Pampaloni and S. Paloscia, Eds., VSP Press, 433–443.

——, and B. M. Lesht, 1996: Measurements of integrated water vapor and cloud liquid water from microwave radiometers at the DOE ARM Cloud and Radiation Testbed in the U.S. Southern Great Plains. *Proc. Int. Geoscience Remote Sensing Symp.* 1996, Lincoln, NE, IEEE, 1675–1677, doi:10.1109/IGARSS.1996.516767.

——, S. A. Boukabara, K. Cady-Pereira, and S. A. Clough, 2005: The effect of the half-width of the 22-GHz water vapor line on retrievals of temperature and water vapor profiles with a 12-channel microwave radiometer. *IEEE Trans. Geosci. Remote Sens.*, **43**, 1102–1108, doi:10.1109/TGRS.2004.839593.

Liou, Y., Y. Teng, T. Van Hove, and J. C. Liljegren, 2001: Comparison of precipitable water vapor observations in the near tropics by GPS, microwave radiometer, and radiosondes. *J. Appl. Meteor.*, **40**, 5–15, doi:10.1175/1520-0450(2001)040<0005:COPWOI>2.0.CO;2.

Löhnert, U., D. D. Turner, and S. Crewell, 2009: Ground-based temperature and humidity profiling using spectral infrared and microwave observations. Part I: Simulated retrieval performance in clear-sky conditions. *J. Appl. Meteor. Climatol.*, **48**, 1017–1032, doi:10.1175/2008JAMC2060.1.

Mace, G. G., T. P. Ackerman, P. Minnis, and D. F. Young, 1998: Cirrus layer microphysical properties derived from surface-based millimeter radar and infrared interferometer data. *J. Geophys. Res.*, **103**, 23 207–23 216, doi:10.1029/98JD02117.

Mather, J. H., D. D. Turner, and T. P. Ackerman, 2016: Scientific maturation of the ARM Program. *The Atmospheric Radiation Measurement (ARM) Program: The First 20 Years, Meteor. Monogr.*, No. 57, Amer. Meteor. Soc., doi:10.1175/AMSMONOGRAPHS-D-15-0053.1.

Mattioli, V., E. R. Westwater, S. I. Gutman, and V. R. Morris, 2005: Forward model studies of water vapor using scanning microwave radiometers, global positioning system, and radiosondes during the Cloudiness Intercomparison Experiment. *IEEE Trans. Geosci. Remote Sens.*, **43**, 1012–1021, doi:10.1109/TGRS.2004.839926.

——, ——, D. Cimini, J. Liljegren, B. M. Lesht, S. I. Gutman, and F. J. Schmidlin, 2007: Analysis of radiosonde and ground-based remotely sensed PWV data from the 2004 North Slope of Alaska Arctic Winter Radiometric Experiment. *J. Atmos. Oceanic Technol.*, **24**, 415–431, doi:10.1175/JTECH1982.1.

——, ——, ——, A. J. Gasiewski, M. Klein, and V. Leuski, 2008: Microwave and millimeter-wave radiometric and radiosonde observations in an arctic environment. *J. Atmos. Oceanic Technol.*, **25**, 1768–1777, doi:10.1175/2008JTECHA1078.1.

May, P., R. Strauch, and K. Moran, 1988: The altitude coverage of temperature measurements using RASS with wind profiling radars. *Geophys. Res. Lett.*, **15**, 1381–1384, doi:10.1029/GL015i012p01381.

McCord, R., and J. W. Voyles, 2016: The ARM data system and archive. *The Atmospheric Radiation Measurement (ARM) Program: The First 20 Years, Meteor. Monogr.,* No. 57, Amer. Meteor. Soc., doi:10.1175/AMSMONOGRAPHS-D-15-0043.1.

McFarlane, S. A., J. H. Mather, and E. J. Mlawer, 2016: ARM's progress on improving atmospheric broadband radiative fluxes and heating rates. *The Atmospheric Radiation Measurement (ARM) Program: The First 20 Years, Meteor. Monogr., No. 57, Amer. Meteor. Soc.*, doi:10.1175/AMSMONOGRAPHS-D-15-0046.1.

Michalsky, J. J., J. C. Liljegren, and L. C. Harrison, 1995: A comparison of Sun photometer derivations of total column water vapor and ozone to standard measures of same at the Southern Great Plains Atmospheric Radiation Measurement site. *J. Geophys. Res.*, **100**, 25 995–26 003, doi:10.1029/95JD02706.

Miller, N. E., J. C. Liljegren, T. R. Shippert, S. A. Clough, and P. D. Brown, 1994: Quality measurement experiments within the Atmospheric Radiation Measurement Program. *Proc. Fourth Atmospheric Radiation Measurement (ARM) Science Team Meeting*, Charleston, SC, U.S. DOE, 5–9. [Available online at http://www.arm.gov/publications/proceedings/conf04/extended_abs/miller_ne.pdf?id=49.]

Miloshevich, L. M., H. Vömel, D. N. Whiteman, B. M. Lesht, F. J. Schmidlin, and F. Russo, 2006: Absolute accuracy of water vapor measurements from six operational radiosonde types launched during AWEX-G and implications for AIRS validation. *J. Geophys. Res.*, **111**, D09S10, doi:10.1029/2005JD006083.

——, ——, ——, and T. Leblanc, 2009: Accuracy assessment and correction of Vaisala RS92 radiosonde water vapor measurements. *J. Geophys. Res.*, **114**, D11305, doi:10.1029/2008JD011565.

Mlawer, E. J., and D. D. Turner, 2016: Spectral radiation measurements and analysis in the ARM Program. *The Atmospheric Radiation Measurement (ARM) Program: The First 20 Years, Meteor. Monogr.*, No. 57, Amer. Meteor. Soc., doi:10.1175/AMSMONOGRAPHS-D-15-0027.1.

——, V. H. Payne, J.-L. Moncet, J. S. Delamere, M. J. Alvarado, and D. C. Tobin, 2012: Development and recent evaluation of the MT_CKD model of continuum absorption. *Philos. Trans. Roy. Soc. London*, **A370**, 2520–2556, doi:10.1098/rsta.2011.0295.

Niell, A. E., 1996: Global mapping functions for the atmosphere delay at radio wavelengths. *J. Geophys. Res.*, **101**, 3227–3246, doi:10.1029/95JB03048.

——, A. J. Coster, F. S. Solheim, V. B. Mendes, P. C. Toor, R. B. Langely, and C. A. Upham, 2001: Comparison of measurements of atmospheric wet delay by radiosonde, water vapor radiometer, GPS, and VLBI. *J. Atmos. Oceanic Technol.*, **18**, 830–850, doi:10.1175/1520-0426(2001)018<0830:COMOAW>2.0.CO;2.

Payne, V. H., J. S. Delamere, K. E. Cady-Pereira, R. R. Gamache, J.-L. Moncet, E. J. Mlawer, and S. A. Clough, 2008: Air-broadened half-widths of the 22 GHz and 183 GHz water vapor lines. *IEEE Trans. Geosci. Remote Sens.*, **46**, 3601–3617, doi:10.1109/TGRS.2008.2002435.

——, E. J. Mlawer, K. E. Cady-Pereira, and J.-L. Moncet, 2011: Water vapor continuum absorption in the microwave. *IEEE Trans. Geosci. Remote Sens.*, **49**, 2194–2208, doi:10:1109/TGRS.2010.2091416.

Racette, P. E., and Coauthors, 2005: Measurement of low amounts of precipitable water vapor using ground-based millimeterwave radiometry. *J. Atmos. Oceanic Technol.*, **22**, 317–337, doi:10.1175/JTECH1711.1.

Revercomb, H. E., H. Buijs, H. B. Howell, D. D. LaPorte, W. L. Smith, and L. A. Sromovsky, 1988: Radiometric calibration of IR Fourier transform spectrometers: Solution to a problem with the High-Resolution Interferometer Sounder. *Appl. Opt.*, **27**, 3210–3218, doi:10.1364/AO.27.003210.

——, and Coauthors, 2003: The Atmospheric Radiation Measurement Program's water vapor intensive observation periods: Overview, accomplishments, and future challenges. *Bull. Amer. Meteor. Soc.*, **84**, 217–236, doi:10.1175/BAMS-84-2-217.

Richardson, S. J., M. E. Splitt, and B. M. Lesht, 2000: Enhancement of ARM surface meteorological observations during the fall 1996 water vapor intensive observation period. *J. Atmos. Oceanic Technol.*, **17**, 312–322, doi:10.1175/1520-0426(2000)017<0312:EOASMO>2.0.CO;2.

Rocken, C., S. Sokolovskiy, J. M. Johnson, and D. Hunt, 2001: Improved mapping of tropospheric delays. *J. Atmos. Oceanic Technol.*, **18**, 1205–1213, doi:10.1175/1520-0426(2001)018<1205:IMOTD>2.0.CO;2.

Rosenkranz, P. W., 1998: Water vapor continuum absorption: A comparison of measurements and models. *Radio Sci.*, **33**, 919–928, doi:10.1029/98RS01182.

Rothacher, M., 1992: Orbits of satellite systems in space geodesy. Ph.D. thesis, University of Bern, 243 pp.

Rothman, L. S., and Coauthors, 1992: The HITRAN molecular database: Editions of 1991 and 1992. *J. Quant. Spectrosc. Radiat. Transfer*, **48**, 469–507, doi:10.1016/0022-4073(92)90115-K.

——, and Coauthors, 2005: The HITRAN 2004 molecular spectroscopic database. *J. Quant. Spectrosc. Radiat. Transfer*, **96**, 139–204, doi:10.1016/j.jqsrt.2004.10.008.

Schmid, B., and Coauthors, 2001: Comparison of columnar water-vapor measurements from solar transmittance methods. *Appl. Opt.*, **40**, 1886–1896, doi:10.1364/AO.40.001886.

Shupe, M. D., J. M. Comstock, D. D. Turner, and G. G. Mace, 2016: Cloud property retrievals in the ARM Program. *The Atmospheric Radiation Measurement (ARM) Program: The First 20 Years, Meteor. Monogr.*, No. 57, Amer. Meteor. Soc., doi:10.1175/AMSMONOGRAPHS-D-15-0030.1.

Smith, T. L., S. G. Benjamin, S. I. Gutman, and S. R. Sahm, 2007: Forecast impact from assimilation of the GPS-IPW observations into the Rapid Update Cycle. *Mon. Wea. Rev.*, **135**, 2914–2930, doi:10.1175/MWR3436.1.

Smith, W. L., and Coauthors, 1981: First sounding results from VAS-D. *Bull. Amer. Meteor. Soc.*, **62**, 232–236.

——, and Coauthors, 1990: GAPEX: A Ground-Based Atmospheric Profiling Experiment. *Bull. Amer. Meteor. Soc.*, **71**, 310–318, doi:10.1175/1520-0477(1990)071<0310:GAGBAP>2.0.CO;2.

——, W. F. Feltz, R. O. Knuteson, H. E. Revercomb, H. M. Woolf, and H. B. Howell, 1999: The retrieval of planetary boundary layer structure using ground-based infrared spectral radiance observations. *J. Atmos. Oceanic Technol.*, **16**, 323–333, doi:10.1175/1520-0426(1999)016<0323:TROPBL>2.0.CO;2.

Soden, B. J., D. D. Turner, B. M. Lesht, and L. M. Miloshevich, 2004: An analysis of satellite, radiosonde, and lidar observations of upper tropospheric water vapor from the Atmospheric Radiation Measurement Program. *J. Geophys. Res.*, **109**, D04105, doi:10.1029/2003JD003828.

Solheim, F. S., J. R. Godwin, and R. Ware, 1998a: Passive, ground-based remote sensing of temperature, water vapor, and cloud liquid profiles by a frequency-synthesized microwave radiometer. *Meteor. Z.*, **7**, 370–376.

——, ——, ——, E. R. Westwater, and Y. Han, 1998b: Radiometric temperature, water vapor, and cloud liquid water profiling with various inversion methods. *Radio Sci.*, **33**, 393–404, doi:10.1029/97RS03656.

Stamnes, K., R. G. Ellingson, J. A. Curry, J. E. Walsh, and B. D. Zak, 1999: Review of science issues, deployment strategy, and status for the ARM North Slope of Alaska – Adjacent Arctic Ocean climate research site. *J. Climate*, **12**, 46–63, doi:10.1175/1520-0442-12.1.46.

Stankov, B. B., E. Gossard, and E. R. Westwater, 1996: High vertical resolution humidity profiling from combined remote sensors. *J. Atmos. Oceanic Technol.*, **13**, 1285–1290, doi:10.1175/1520-0426(1996)013<1285:UOWPEO>2.0.CO;2.

Stokes, G. M., 2016: Original ARM concept and launch. *The Atmospheric Radiation Measurement (ARM) Program: The First 20 Years, Meteor. Monogr.*, No. 57, Amer. Meteor. Soc., doi:10.1175/AMSMONOGRAPHS-D-15-0021.1.

Suomi, V. E., and T. H. Vonder Haar, 1969: Geosynchronous meteorological satellite. *J. Spacecr.*, **6**, 342–344, doi:10.2514/3.29604.

Tobin, D. C., and Coauthors, 1999: Downwelling spectral radiance observations at the SHEBA ice station: Water vapor continuum measurements from 17 to 26 μm. *J. Geophys. Res.*, **104**, 2081–2092, doi:10.1029/1998JD200057.

——, and Coauthors, 2006: Atmospheric Radiation Measurement site atmospheric state best estimates for Atmospheric Infrared Sounder temperature and water vapor retrieval validation. *J. Geophys. Res.*, **111**, D09S14, doi:10.1029/2005JD006103.

Turner, D. D., 2008: Ground-based retrievals of optical depth, effective radius, and composition of airborne mineral dust above the Sahel. *J. Geophys. Res.*, **113**, D00E03, doi:10.1029/2008JD010054.

——, and J. E. M. Goldsmith, 1999: Twenty-four-hour Raman lidar water vapor measurements during the Atmospheric Radiation Measurement Program's 1996 and 1997 water vapor intensive observation periods. *J. Atmos. Oceanic Technol.*, **16**, 1062–1076, doi:10.1175/1520-0426(1999)016<1062:TFHRLW>2.0.CO;2.

——, and E. J. Mlawer, 2010: The Radiative Heating in Underexplored Bands Campaigns (RHUBC). *Bull. Amer. Meteor. Soc.*, **91**, doi:10.1175/2010BAMS2904.1.

——, and U. Löhnert, 2014: Retrieving temperature and humidity profiles from the ground-based Atmospheric Emitted Radiance Interferometer (AERI). *J. Appl. Meteor. Climatol.*, **53**, 752–771, doi:10.1175/JAMC-D-13-0126.1.

——, W. F. Feltz, and R. A. Ferrare, 2000: Continuous water vapor profiles from operational ground-based active and passive remote sensors. *Bull. Amer. Meteor. Soc.*, **81**, 1301–1317, doi:10.1175/1520-0477(2000)081<1301:CWBPFO>2.3.CO;2.

——, R. A. Ferrare, L. A. Heilman Brasseur, W. F. Feltz, and T. P. Tooman, 2002: Automated retrievals of water vapor and aerosol profiles from an operational Raman lidar. *J. Atmos. Oceanic Technol.*, **19**, 37–50, doi:10.1175/1520-0426(2002)019<0037:AROWVA>2.0.CO;2.

——, S. A. Ackerman, B. A. Baum, H. E. Revercomb, and P. Yang, 2003a: Cloud phase determination using ground-based AERI observations at SHEBA. *J. Appl. Meteor.*, **42**, 701–715, doi:10.1175/1520-0450(2003)042<0701:CPDUGA>2.0.CO;2.

——, B. M. Lesht, S. A. Clough, J. C. Liljegren, H. E. Revercomb, and D. C. Tobin, 2003b: Dry bias and variability in Vaisala radiosondes: The ARM experience. *J. Atmos. Oceanic Technol.*, **20**, 117–132, doi:10.1175/1520-0426(2003)020<0117:DBAVIV>2.0.CO;2.

——, and Coauthors, 2004: The QME AERI LBLRTM: A closure experiment for downwelling high spectral resolution infrared radiance. *J. Atmos. Sci.*, **61**, 2657–2675, doi:10.1175/JAS3300.1.

——, R. O. Knuteson, H. E. Revercomb, C. Lo, and R. G. Dedecker, 2006: Noise reduction of Atmospheric Emitted Radiance Interferometer (AERI) observations using principal component analysis. *J. Atmos. Oceanic Technol.*, **23**, 1223–1238, doi:10.1175/JTECH1906.1.

——, S. A. Clough, J. C. Liljegren, E. E. Clothiaux, K. Cady-Pereira, and K. L. Gaustad, 2007: Retrieving liquid water path and precipitable water vapor from the Atmospheric Radiation Measurement (ARM) microwave radiometers. *IEEE Trans. Geosci. Remote Sens.*, **45**, 3680–3690, doi:10.1109/TGRS.2007.903703.

——, U. Löhnert, M. Cadeddu, S. Crewell, and A. Vogelmann, 2009: Modifications to the water vapor continuum in the microwave suggested by ground-based 150-GHz observations. *IEEE Trans. Geosci. Remote Sens.*, **47**, 3326–3337, doi:10.1109/TGRS.2009.2022262.

——, A. Merrelli, D. Vimont, and E. J. Mlawer, 2012: Impact of modifying the longwave water vapor continuum absorption model on community Earth system model simulations. *J. Geophys. Res.*, **117**, D04106, doi:10.1029/2011JD016440.

——, J. E. M. Goldsmith, and R. A. Ferrare, 2016: Development and applications of the ARM Raman lidar. *The Atmospheric Radiation Measurement (ARM) Program: The First 20 Years, Meteor. Monogr.*, No. 57, Amer. Meteor. Soc., doi:10.1175/AMSMONOGRAPHS-D-15-0026.1.

Verlinde, J., B. Zak, M. D. Shupe, M. Ivey, and K. Stamnes, 2016: The ARM North Slope of Alaska (NSA) sites. *The Atmospheric Radiation Measurement (ARM) Program: The First 20 Years, Meteor. Monogr.*, No. 57, Amer. Meteor. Soc., doi:10.1175/AMSMONOGRAPHS-D-15-0023.1.

Vömel, H., and Coauthors, 2007: Radiation dry bias of the Vaisala RS92 humidity sensor. *J. Atmos. Oceanic Technol.*, **24**, 953–963, doi:10.1175/JTECH2019.1.

Vonder Haar, T. H., and V. E. Suomi, 1971: Measurements of the Earth's radiation budget from satellites during a five-year period. Part I: Extended time and space means. *J. Atmos. Sci.*, **28**, 305–314, doi:10.1175/1520-0469(1971)028<0305:MOTERB>2.0.CO;2.

Wade, C. G., 1994: An evaluation of problems affecting the measurement of low relative humidity on the U.S. radiosonde. *J. Atmos. Oceanic Technol.*, **11**, 687–700, doi:10.1175/1520-0426(1994)011<0687:AEOPAT>2.0.CO;2.

Wagner, T. J., W. F. Feltz, and S. A. Ackerman, 2008: The temporal evolution of convective indices in storm-producing environments. *Wea. Forecasting*, **23**, 786–794, doi:10.1175/2008WAF2007046.1.

——, D. D. Turner, L. K. Berg, and S. K. Krueger, 2013: Ground-based remote retrievals of cumulus entrainment rates. *J. Atmos. Oceanic Technol.*, **30**, 1460–1471, doi:10.1175/JTECH-D-12-00187.1.

Wang, J., H. L. Cole, D. J. Carlson, E. R. Miller, K. Beierle, A. Paukkunen, and T. K. Laine, 2002: Corrections of humidity measurement errors from the Vaisala RS80 radiosonde—Application to TOGA COARE data. *J. Atmos. Oceanic Technol.*, **19**, 981–1002, doi:10.1175/1520-0426(2002)019<0981:COHMEF>2.0.CO;2.

Ware, R., R. Carpenter, J. Güldner, J. C. Liljegren, T. Nehrkorn, F. Solheim, and F. Vandenberghe, 2003: A multichannel radiometric profiler of temperature, humidity, and cloud liquid. *Radio Sci.*, **38**, 8079, doi:10.1029/2002RS002856.

Westwater, E. R., 1997: Remote sensing of tropospheric temperature and water vapor by integrated observing systems. *Bull. Amer. Meteor. Soc.*, **78**, 1991–2006.

Whiteman, D. N., S. H. Melfi, and R. A. Ferrare, 1992: Raman lidar system for measurement of water vapor and aerosols in the Earth's atmosphere. *Appl. Opt.*, **31**, 3068–3082, doi:10.1364/AO.31.003068.

Wolfe, D. E., and S. I. Gutman, 2000: Developing an operational, surface-based, GPS, water vapor observing system for NOAA: Network design and results. *J. Atmos. Oceanic Technol.*, **17**, 426–439, doi:10.1175/1520-0426(2000)017<0426:DAOSBG>2.0.CO;2.

Wulfmeyer, V., and Coauthors, 2011: The Convective and Orographically-induced Precipitation Study (COPS): The scientific strategy, the field phase, and research highlights. *Quart. J. Roy. Meteor. Soc.*, **137**, 3–30, doi:10.1002/qj.752.

Zhang, M. H., and J. L. Lin, 1997: Constrained variational analysis of sounding data based on column-integrated budgets of mass, heat, moisture, and momentum: Approach and application to ARM measurements. *J. Atmos. Sci.*, **54**, 1503–1524, doi:10.1175/1520-0469(1997)054<1503:CVAOSD>2.0.CO;2.

——, ——, R. T. Cederwall, J. J. Yio, and S. C. Xie, 2001: Objective analysis of ARM IOP data: Method and sensitivity. *Mon. Wea. Rev.*, **129**, 295–311, doi:10.1175/1520-0493(2001)129<0295:OAOAID>2.0.CO;2.

——, R. C. J. Somerville, and S. Xie, 2016: The SCM concept and creation of ARM forcing datasets. *The Atmospheric Radiation Measurement (ARM) Program: The First 20 Years, Meteor. Monogr.*, No. 57, Amer. Meteor. Soc., doi:10.1175/AMSMONOGRAPHS-D-15-0040.1.